Composites of Oxidized Boron Carbonitride Nanotubes with Polyaniline: Preparation and Conductivity Studies

Ye-yong Meng, Zheng Zhu, Sheng-Jun Zhou, Su-Yuan Xie, Rong-Bin Huang,* and Lan-Sun Zheng

State Key Laboratory for Physical Chemistry of Solid Surfaces and Department of Chemistry, College of Chemistry and Chemical Engineering, Xiamen University, Xiamen, 361005 China

Received: January 20, 2010; Revised Manuscript Received: July 4, 2010

Five precursors of boron carbonitride nanotubes with different B/N ratios were synthesized. Oxidation with nitric acid afforded oxidized boron carbonitride nanotubes (o-BCNNTs), with which composites with polyaniline (o-BCNNTs/PANI) were prepared by in situ oxidative polymerization. For one of the o-BCNNTs, composites were synthesized with a varying amount of the nanotube (up to 30 wt %), while for the rest the nanotube content was maintained at 30 wt % in each case. It has been found that the conductivity of the oxidized boron carbonitride nanotubes decreases with an increasing B/N ratio and that of the composites increases with an increasing percentage of the o-BCNNTs.

1. Introduction

Composites of carbon nanotubes (CNTs) with polymers have attracted much recent interest due to their unique electronic and mechanical properties.[1−11] As a filling material in composites, CNTs offer many useful properties, in particular their electronic properties and mechanical strength.[12] However, fabricating CNT-based electronic materials has been a great challenge as the nanotubes' electronic properties, being a conductor or semiconductor, are sensitively dependent on the tube diameter and chirality, the control of which remains a formidable challenge.[13]

It is thus not surprising that great efforts have been pursued to explore alternatives to CNTs and their applications in making processable electronic materials. One such nanotubular material is ternary boron carbonitride nanotubes (BCNNTs). They are of interest, not only because of their unique electronic properties, but also because of the relative ease in fine-tuning such properties.[14,15] Theoretical studies have predicted that the band gap of BCNNTs may be tailored over a wide range by changing their chemical composition rather than being dictated by the geometric structure as in the case of CNTs.[16−18] BCNNTs are therefore promising alternatives to CNTs for the making of polymer composites with potential electronic applications.

In making BCNNT/polymer composites, there are two main challenges: poor solubility of BCNNTs in typical organic solvents and their incompatibility with polymers. The most straightforward solution is to chemically modify the nanotube surface. With the functional groups introduced, the rope structure of the nanotubes is easily disrupted and interactions of the modified nanotubes with solvents are greatly improved. Surface functionalization of BCNNTs readily benefits from analogous research with CNTs, which has been perfected over the past years.[6−11] For example, oxidation of CNTs with nitric acid has provided derivatives featuring carboxylic acid groups onto the open ends and surface defect sites of CNTs.[19,20]

In this contribution, we have succeeded in making composites of oxidized boron carbonitride nanotubes with polyaniline[21] (o-BCNNTs/PANI). Composites of various combinations of o-BCNNTs and PANI have been made, and their electrical conductivities have been measured. The relationship between the conductivity of an o-BCNNT and its B/N ratio and the relationship between the conductivity of the composite and its o-BCNNT content are established.

2. Experimental Section

2.1. Raw Materials. Multiwalled carbon nanotubes (MWCNTs) were purchased from Shenzhen Nanotech Port Co. Ltd. Aniline hydrochloride (99%) was purchased from Alfa Aesar. Other solvents and compounds were purchased from Sinopharm Chemical Reagent Co. Ltd. All chemicals were used as received.

2.2. Syntheses of o-BCNNTs/PANI Composites. The synthesis of o-BCNNTs/PANI composites, involving (1) the formation of BCNNTs, (2) surface modification of BCNNTs, and (3) attachment of PANI onto the surface-functionalized BCNNTs, is shown in Scheme 1.

2.2.1. Synthesis of BCNNTs. A mixture of commercially obtained CNTs (0.40 g), H_3BO_3 (0.52 g), and anhydrous ammonia in a quartz tube was heated at 1080 °C for 6 h. BCNNTs with five different B/N ratios were obtained by controlling the flow rate of ammonia (i.e., 100, 120, 150, 180, and 200 mL/min).

2.2.2. Oxidation of BCNNTs. The as-synthesized BCNNTs were ultrasonically dispersed in 14.6 M nitric acid, and the mixture was maintained under reflux for 12 h. After cooling to room temperature, the reaction mixture was subject to centrifugation (8000 rpm for 5 min). The solid was collected, washed with deionized water (10 mL × 3), and vacuum filtered using a 0.45-μm-pore-size polycarbonate filter membrane. The products were then dried in an oven at 313 K for 6 h. The oxidized samples obtained using the five different BCNNTs mentioned above were designated as S1, S2, S3, S4, and S5, respectively.

2.2.3. Preparation of o-BCNNTs/PANI Composites. The third sample of o-BCNNTs (S3) was selected for examining the effect of percentage of o-BCNNTs. A sample of S3 (0.0213 g) was ultrasonically dispersed in 10 mL of HCl solution (aqueous 1 M), to which a solution of aniline (0.4264 g) in 10

* Corresponding author. E-mail: rbhuang@xmu.edu.cn.

10.1021/jp100541j
Published on Web 07/22/2010

SCHEME 1: Synthesis of o-BCNNTs/PANI Composites

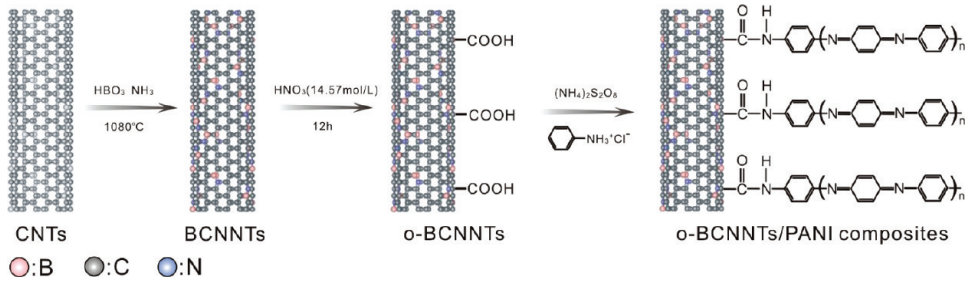

mL of HCl solution (aqueous 1 M) was added. To this mixture was quickly added a freshly prepared solution of ammonium peroxydisulfate (0.18 g dissolved in10 mL of HCl solution (aqueous 1 M), and the mixture thus obtained was shaken vigorously for 30 s. A dark green suspension was obtained after a few minutes, indicating the formation of polyaniline. The mixture was then filtered, and the precipitate was washed with a HCl solution (0.5 mM) and dried under vacuum at room temperature for 24 h.

While keeping the amount of aniline constant, five different amounts of S3 (0, 5, 10, 15, and 30 wt % o-BCNNTs based on the weight of aniline) were utilized to make the o-BCNNT/PANI composites. Using S1, S2, S4, and S5 (in each case 30 wt % with respect to the amount of aniline), o-BCNNTs/PANI composites were also prepared, and are designated as C1, C2, C4, and C5, respectively.

2.3. Characterization of Materials. The morphologies and structures of the products were characterized by field emission scanning electron microscopy (FE-SEM, LEO1530) equipped with energy-dispersive X-ray (EDX) and high-resolution transmission electron microscopy (HRTEM, TECNAI F-30) with an accelerating voltage of 300 kV. The compositions and functional groups of the products were identified by powder X-ray diffraction (XRD), Raman spectroscopy, and Fourier transform infrared (FT-IR) spectroscopy. The XRD spectra were acquired by using a Panalytical X-pert diffractometer with copper Kα radiation. Raman spectra of the CNTs, raw BCNNTs, and o-BCNNTs were recorded using a Labram I confocal microprobe Raman system (Dilor, France). A Spectra Physics He−Ne laser, operating at 632 nm with a power of about 4 mW on the sample, was used in the experiment. The FT-IR spectra were measured with a Nicolet Avatar 330 FT-IR spectrometer using a KBr pellet. The conductivity measurements were carried out by the four-probe technique (SX1934(SZ-82)) at room temperature.

3. Results and Discussion

3.1. Characterization of Synthesized Composites. In this work, BCNNTs were synthesized by the carbon nanotube substitution reaction using boric acid and anhydrous ammonia, followed by oxidation with HNO_3. By controlling the flow rate of anhydrous ammonia, the B/N ratio of the modified nanotubes can be tuned. The BCNNTs before and after oxidization were characterized. Figure 1 shows the morphology and elemental

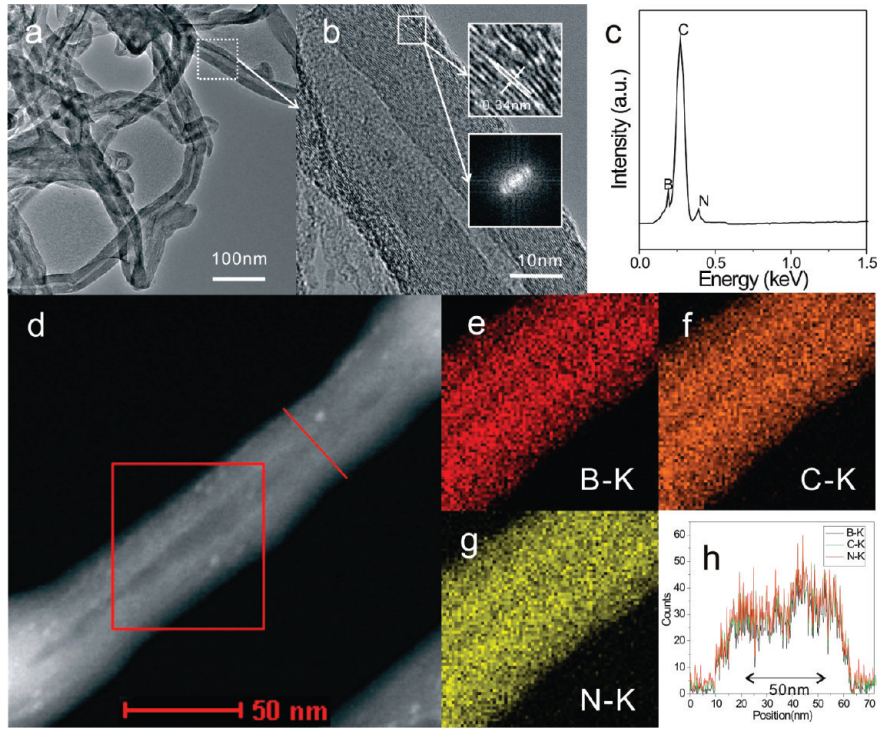

Figure 1. (a) Typical low-magnification TEM image, (b) HRTEM image, and (c) EDX spectrum of raw BCNNTs; (d) STEM image of an individual raw BCNNT; (e−g) elemental maps of B, C, and N in the part of the BCNNT marked with the rectangle in (d); (h) cross-sectional compositional line profiles of the raw BCNNT (indicated by a line in Figure 1d). The insets in (b) are the HRTEM image and the corresponding FFT pattern of the area marked with the square.

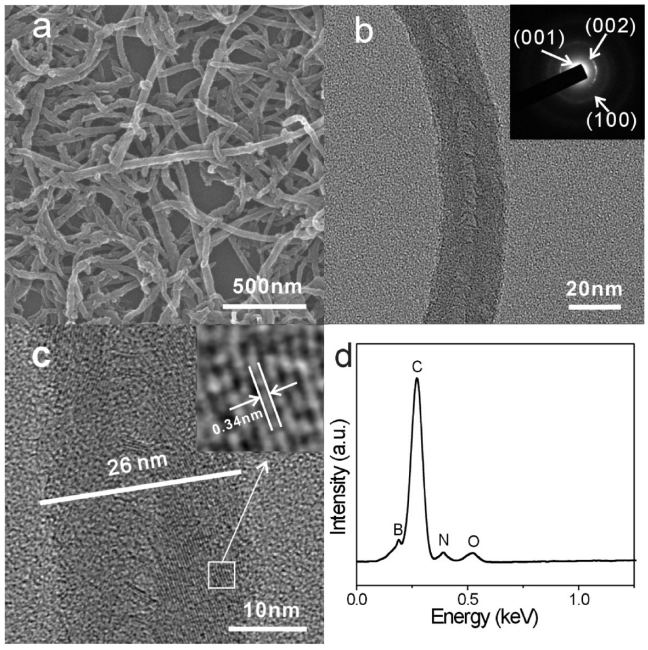

Figure 2. (a) Typical large-area SEM image of o-BCNNTs; (b) typical low-magnification TEM image; (c) HRTEM image; (d) EDS spectrum of an individual o-BCNNT. Inset in (b) is the corresponding SAED pattern.

compositions of the raw BCNNTs prepared at 150 mL/min flow rate of anhydrous ammonia. From Figure 1a, it can be seen that the as-prepared BCNNTs retain a well-define tubular structure with diameters ranging from 20 to 50 nm. The corresponding HRTEM image (Figure 1b) shows that the nanotube wall exhibits well-defined lattice fringes with a spacing of 0.34 nm, similar to the (002) plane of graphite. The bright spots in the corresponding fast Fourier transform (FFT) pattern reveal good crystallinity of the nanotubes. The composition of these nanotubes was further confirmed by an EDX spectrum (Figure 1c), indicating that the as-prepared BCNNT contains B (17 wt %), N (10 wt %), and C (73 wt %). Both the element maps (Figure 1d−g) and the cross-sectional compositional line profiles further demonstrate that B, C, and N atoms are uniformly distributed in the BCNNTs. Based on the above EDS analysis, it can be concluded that the reaction of CNTs with H_3BO_3 and NH_3 can be used as a general route to prepare BCNNTs wherein carbon atoms of CNTs are partially substituted by B and N atoms without topological changes of the original tubular structure.

The morphology and structural features of the oxidized BCNNTs (o-BCNNTs) are shown in Figure 2. The o-BCNNTs appear to keep the same morphology as the unmodified BCNNTs, as indicated by Figure 2a−c. However, the corresponding SAED pattern (the inset of Figure 2b) reveals that the wall crystallinity was deteriorated after the treatment with HNO_3, as the diffraction spots in the pattern are elongated to arcs. Oxygen is detected in the EDS spectrum of the o-BCNNTs (Figure 2d), implying that some O-containing functional groups reside on the surface of the BCNNTs.

Figure 3 shows the electron microscopy images of o-BCNNTs hybridized with PANI. As an example, Figure 3a shows the overall morphology of the product with 5 wt % o-BCNNTs. It can be seen that a large quantity of one-dimensional nanostructures with a smooth surface are well dispersed and isolated. More detailed structural information was provided by TEM characterization. Figure 3b is a low-magnification TEM image, showing a tubular structure of the as-prepared o-BCNNTs (5 wt %)/PANI composite. The corresponding HRTEM image (Figure 3c) clearly shows that the nanotube is covered by a layer of amorphous material, likely PANI polymer, with light diffraction contrast. Interestingly, as shown in Figure 3c−f, the polymer layer seems to become thinner with the increasing amount of o-BCNNTs. When the ratio of the BCNNTs changes from 5 to 30 wt %, the thickness of polymer layer decreases from ca. 10 nm to only 1 nm, but the uniformity of thickness appears to be much improved.

XRD patterns of as-prepared BCNNTs, o-BCNNTs, pure PANI, and composites with various amounts of o-BCNNTs are shown in Figure 4. As shown in curves b−e, diffractions of the

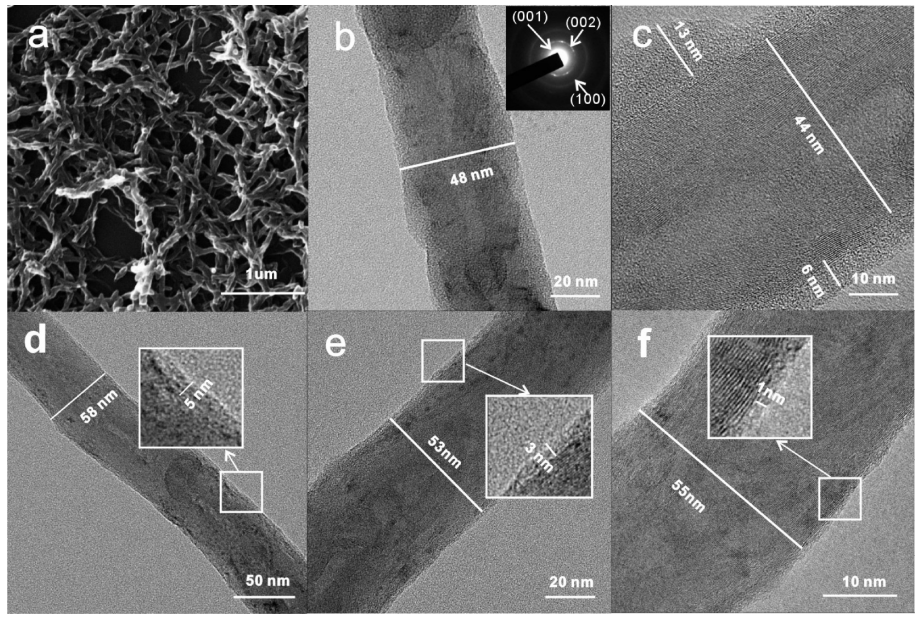

Figure 3. (a) SEM image and (b) TEM image of composites containing 5 wt % o-BCNNTs; typical TEM images of the composites containing (c) 5, (d) 10, (e) 15, and (f) 30 wt % o-BCNNTs. The inset in (b) is the SAED pattern of the composites containing 5 wt % o-BCNNTs, and the insets in (d)−(f) are the HRTEM images of the area marked with the squares.

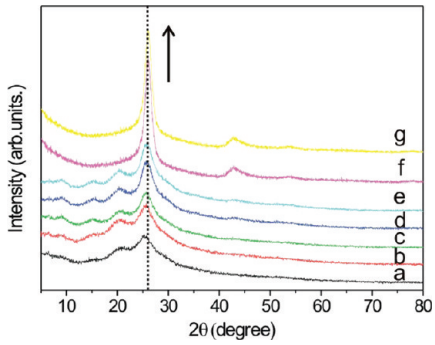

Figure 4. Typical XRD patterns of (a) pure PANI, composites containing (b) 5, (c) 10, (d) 15, and (e) 30 wt % o-BCNNTs, (f) o-BCNNTs, and (g) as-prepared BCNNTs.

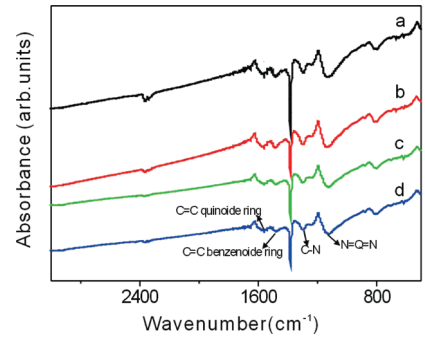

Figure 6. IR spectra of composites containing (a) 5, (b) 10, (c) 15, and (d) 30 wt % o-BCNNTs.

composites generate a number of broad peaks at low angles (9°, 15°, 20°, and 26°). Such pronounced oscillating structures are due to the periodic structure of PANI, indicating in the composites the presence of PANI (ES) with an oxidation degree of 0.5. The XRD peak of the composites at 26° is due to the overlapping of the (200) reflection of PANI and the (001) reflection of BCNNTs,[22] with the intensity of the peak (versus the peak at 26°) increasing proportionally to the increase of o-BCNNTs in starting materials. This observation is consistent with the changing trend in the thickness of the PANI layer when the amount of o-BCNNTs increases and that of PANI decreases in the composites.

The experimental results have demonstrated that o-BCNNTs are covered by the PANI to form a core−shell composite structure. Mechanistically, it may be understood that the crucial step of BCNNT oxidation with nitric acid produced carboxyl groups that serve as "NH_2 anchors" as shown in Scheme 1. FT-IR and Raman spectroscopies were used to identify characteristic functional groups of the products obtained at different synthetic stages.

The infrared spectra of CNTs, as-prepared BCNNTs, and o-BCNNTs are shown in Figure 5a. The FT-IR spectrum of CNTs shows the signal of an aromatic C═C vibration at 1579 cm^{-1}. The spectrum of as-prepared BCNNTs shows three sharp IR absorption bands at 800, 1380, and 1630 cm^{-1} with a broad absorption at 1000−1300 cm^{-1}. The absorption bands at 800 and 1380 cm^{-1} are induced by the sp^2-hybridized BN phase. The blue shift of the out-of-plane bending mode to 800 cm^{-1} (usually at 780 cm^{-1}) is due to the increase in bond stiffness, probably induced by the incorporation of non-BN bonds in the hexagonal network. The absorption band at 1630 cm^{-1} is due to the presence of C═N bonds.[23] The broad absorption at 1000−1300 cm^{-1} may be induced by sp^3-bonded B−N (at 1060−1090 cm^{-1})[24] or boron carbide bonds (1100−1250 cm^{-1}).[25] In the IR spectrum of o-BCNNTs, there is a band at 1235 cm^{-1} due to C−OR groups and a considerable increase in the intensity of the bands at 1580 and 1720 cm^{-1}, because of the presence of C═O.

The Raman spectra of CNTs, as-prepared BCNNTs, and o-BCNNTs are shown in Figure 5b. These spectra show BCNNTs possess a Raman signal with two strong bands at ∼1568 and ∼1318 cm^{-1}, known as the G (graphite) and D (disorder) bands that represent zone center phonons of E_{2g} symmetry and K-point phonons of A_{1g} symmetry, respectively.[26] For the CNTs, the intensity of the G band is stronger than that of the D band. However, the intensity of the D band increases after conversion to the BCNNTs, so much so that its intensity exceeds that of the G band. The intensity ratio between the D and G bands (I_D/I_G) is estimated to be 1.32, indicating the presence of graphite nanoclusters.[25] This result means that the carbon phase in BCNNTs is separated from the sp^2-BN phase as graphite nanoclusters. In addition, the G peak of BCNNTs is higher in wavenumber than the corresponding peak in the CNTs. The above results show that most of the carbon atoms in these nanotubes do not bond in a stable graphite phase, most likely due to the bond hybridization with B and N atoms. Compared with the as-prepared BCNNTs, the I_D/I_G of o-BCNNTs is further enhanced. It can be seen that the oxidation treatment by HNO_3 is harmful to the crystallinity of the tubular structure.

The IR spectra of the four composites (5, 10, 15, and 30 wt % concentration of o-BCNNTs) are shown in Figure 6. The absorptions at 1550−1600 and 1465 cm^{-1} are related to C═C groups of the quinoid ring and C═C groups of the benzenoid ring, respectively. The band at 1300 cm^{-1} is

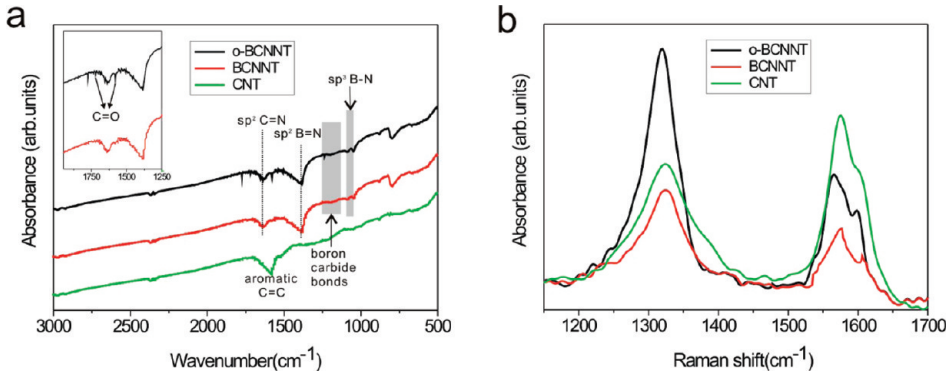

Figure 5. (a) IR spectra and (b) Raman spectra (λ_{laser} = 632 nm) of CNTs, as-prepared BCNNTs, and o-BCNNTs.

TABLE 1: Molecular Composition of o-BCNNTs

sample	C	B	N	O	B + N
S1	78	16	1	5	17
S2	76	14	5	5	19
S3	73	17	6	4	23
S4	70	17	8	5	25
S5	67	17	11	5	28

assigned to C−N bonds of secondary aromatic amines. The band at 1130 cm^{-1} corresponds to the N=Q=N bond. It reflects the degree of electronic delocalization, and it is characteristic of PANI conductivity.[27] This may suggest that the strong interactions between o-BCNNTs and PANI facilitates electronic delocalization, thus enhancing the electrical conductivity of the polymeric chains. The presence of these bands confirms the presence of the doped form of PANI in composites. In addition, it should be mentioned that the IR absorption assigned to PANI appreciably decreases in intensity with the increase of the feeding ratio of the o-BCNNTs to aniline monomer. This result agrees well with the thickness-changing trend of the PANI coating layer revealed above by the TEM characterization.

3.2. Conductivity of Oxidized BCNNTs. The chemical compositions based on EDS measurement of S1−S5 are summarized in Table 1. With the increasing flow rate of ammonia, the carbon content decreases while the amount of nitrogen increases from 1 to 11%. It has been shown both theoretically and experimentally that the conductivity of the doped carbon nanotubes is profoundly affected by the ratio of B and N.[12,13] Indeed, as revealed by Figure 7, the conductivity of o-BCNNTs decreases with increasing B + N content in the doped nanotubes. For example, S1 (B + N = 17%) has a conductivity of 6.78 S/cm while the conductivity of S5 (B + N = 28) is 4.85 S/cm.

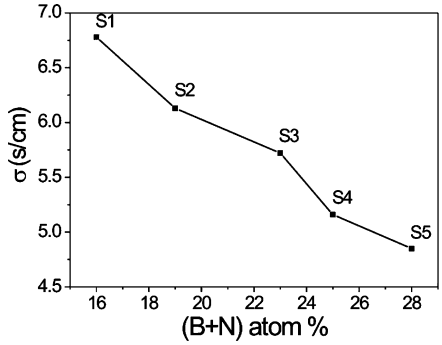

Figure 7. Relationship between conductivity of o-BCNNTs and amount of B + N in the nanotube.

3.3. Conductivity of o-BCNNTs/PANI Composites. Figure 8a shows the conductivity of o-BCNNT/PANI composites as a function of the amount of o-BCNNT (S3) in the composites. The conductivity of pure PANI is only 1.19 S/cm. When the o-BCNNT is present in 5 wt %, the conductivity of the composite increased appreciably, and the conductivity quickly reaches the value 3.51 S/cm when the composite contains 30 wt % o-BCNNTs, beyond which the conductivity of the composite remains constant. Obviously, the conductivity of the o-BCNNT/PANI composite is related to the thickness of the PANI layer covered on the o-BCNNTs, which in turn is inversely proportional to the o-BCNNT/PANI ratio. The composite with 30 wt % o-BCNNTs has a thin PANI layer (only 1 nm). Therefore, this composite has almost the same conductivity as o-BCNNTs. The improved electrical conductivity of the o-BCNNTs/PANI with respect to pure PANI is attributed to functionalized BCNNTs serving as a "conducting bridge" between PANI conducting domains. Compared with traditional CNT/PANI composites, the conductivity of the present o-BCNNT-containing composites can be readily obtained by adjusting the chemical composition of BCNNTs.

Figure 8b shows the change of the composite conductivity containing various o-BCNNT fillers doped at the same percentage (30 wt %). All composites display improved conductivity with respect to pure PANI, but the degree of improvement is highly dependent on the chemical composition of the o-BCNNT with C5, the composite with the highest B + N content being the least conductive one among the five composites studied; the lower amount of C in o-BCNNTs (S5) may have hindered the charge transfer between the nanotubes and PANI.

4. Conclusions

In this study, the o-BCNNT/PANI composites were prepared by surface functionalization of BCNNTs followed by polymerization of aniline on the functionalized surfaces of o-BCNNTs. Depending on the o-BCNNT/aniline ratio, the PANI layer covering the nanotubes and the amount of o-BCNNTs in a particular composite can be tuned. It has been found that the conductivity of the resulting o-BCNNT/PANI composites is greatly enhanced, up to 2 orders of magnitude, with respect to pure PANI, and can be tuned by varying the amount of any particular o-BCNNT filler or through the use of different o-BCNNTs "doped" at the percentage level. Such widely tunable conductivity of the o-BCNNT/PANI composites has potential applications in making electric devices. Most importantly, the results presented herein suggest that BCNNTs are a promising class

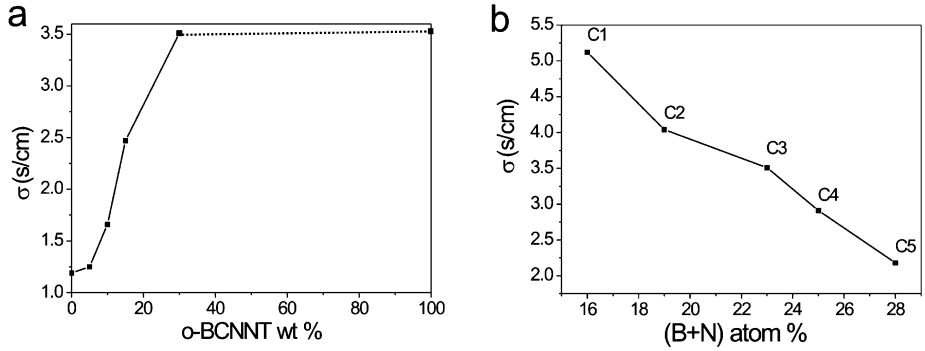

Figure 8. Change of composite conductivity versus (a) amount of any particular o-BCNNT (S3) and (b) chemical composition of various o-BCNNT fillers doped at the same percentage (30 wt %).

of alternative to the well-studied CNTs for making technologically important conductive composites.

Acknowledgment. This work was supported by the National Natural Science Foundation of China (Grants 20721001 and 20525103) and the National Basic Research Program of China (Grant 2007CB815301).

References and Notes

(1) Cooper, C. A.; Young, R. J.; Halsall, M. *Composites, Part A* **2001**, *32A*, 401.

(2) Long, Y. Z.; Yin, Z. H.; Chen, Z. J. *J. Phys. Chem. C* **2008**, *112*, 11507.

(3) Coleman, J. N.; Curran, S.; Dalton, A. B.; Davey, A. P.; McCarthy, B.; Blau, W.; Barklie, R. C. *Synth. Met.* **1999**, *102*, 1174.

(4) Woo, H. S.; Czerw, R.; Webster, S.; Carroll, D. L.; Park, J. W.; Lee, J. H. *Synth. Met.* **2001**, *116*, 369.

(5) MacDiarmid, A. G.; Chiang, J. C.; Halpern, M.; Huang, W. S.; Mu, S. L.; Somasiri, N. L. D.; Wu, W.; Yaniger, S. I. *Mol. Cryst. Liq. Cryst.* **1985**, *121*, 173.

(6) Hiura, H.; Ebbesen, T. W.; Tanigaki, K. *Adv. Mater.* **1995**, *7*, 275.

(7) Satishkumar, B. C.; Govindaraj, A.; Mofokeng, J.; Subbanna, G. N.; Rao, C. N. R. *J. Phys. B* **1996**, *29*, 4925.

(8) Yan, X. B.; Han, Z. J.; Yang, Y.; Tay, B. K. *J. Phys. Chem. C* **2007**, *111*, 4125.

(9) Li, L.; Qin, Z. Y.; Liang, X.; Fan, Q. Q.; Lu, Y. Q.; Wu, W. H.; Zhu, M. F. *J. Phys. Chem. C* **2009**, *113*, 5502.

(10) Liu, J.; Rinzler, A. G.; Dai, H.; Hafner, J. H.; Bradley, R. K.; Boul, P. J.; Lu, A.; Iverson, T.; Shelimov, K.; Huffman, C. B.; Rodriguez-Macias, F.; Shon, Y.-S.; Lee, T. R.; Colbert, D. T.; Smalley, R. E. *Science* **1998**, *280*, 1253.

(11) Zhang, H.; Li, H. X.; Cheng, H. M. *J. Phys. Chem. B* **2006**, *110*, 9095.

(12) Zhang, F.; Xu, Q.; Zhang, H.; Zhang, Z. *J. Phys. Chem. C* **2009**, *113*, 18531.

(13) Zhao, B.; Hu, H.; Niyogi, S.; Itkis, M. E.; Hamon, M. A.; Bhowmik, P.; Meier, M. S.; Haddon, R. C. *J. Am. Chem. Soc.* **2001**, *123*, 11673.

(14) Stephan, O.; Ajayan, P. M.; Colliex, C.; Redlich, P.; Lambert, J. M.; Bernier, P.; Lefin, P. *Science* **1994**, *266*, 1683.

(15) Weng-Sieh, Z.; Cherrey, K.; Chopra, N. G.; Blasé, X.; Miyamoto, Y.; Rubio, A.; Cohen, M. L.; Louie, S. G.; Zettl, A.; Gronsky, R. *Phys. Rev. B* **1995**, *51*, 11229.

(16) Liao, L.; Liu, K.; Wang, W.; Bai, X.; Wang, E.; Liu, Y.; Li, J.; Liu, C. *J. Am. Chem. Soc.* **2007**, *129*, 9562.

(17) Blasé, X.; Charlier, J. C.; De Vita, A.; Car, R. *Appl. Phys. Lett.* **1997**, *70*, 197.

(18) Enyashin, A. N.; Makurin, Y. N.; Ivanovskii, A. L. *Carbon* **2004**, *42*, 2081.

(19) Martinez, M. T.; Callejas, M. A.; Benito, A. M.; Cochet, M.; Seeger, T.; Anson, A.; Schreiber, J.; Gordon, C.; Marhic, C.; Chauvet, O.; Maser, W. K. *Nanotechnology* **2003**, *14*, 691.

(20) Martinez, M. T.; Callejas, M. A.; Benito, A. M.; Cochet, M.; Seeger, T.; Anson, A.; Schreiber, J.; Gordon, C.; Marhic, C.; Chauvet, O.; Fierro, J. L. G.; Maser, W. K. *Carbon* **2003**, *41*, 2247.

(21) Li, D.; Kaner, R. B. *J. Am. Chem. Soc.* **2006**, *128*, 968.

(22) Zhang, L.; Wan, M.; Wei, Y. *Macromol. Rapid Commun.* **2006**, *27*, 366.

(23) Yap, Y. K.; Kida, S.; Aoyama, T.; Mori, Y.; Sasaki, T. *Appl. Phys. Lett.* **1998**, *73*, 915.

(24) Yap, Y. K.; Aoyama, T.; Wada, Y.; Yoshimura, M.; Mori, Y.; Sasaki, T. *Diamond Relat. Mater.* **2000**, *9*, 592.

(25) Wada, Y.; Yap, Y. K.; Yoshimura, M.; Mori, Y.; Sasaki, T. *Diamond Relat. Mater.* **2000**, *9*, 620.

(26) Ferrari, A. C.; Robertson, J. *J. Phys. Rev. B* **2000**, *61*, 14095.

(27) Quillard, S.; Louarn, G.; Lefrant, S.; Macdiarmid, A. G. *Phys. Rev. B* **1994**, *50*, 12498.

JP100541J